

Synthesis and Characterization of Polystyrene Composites with Oxidized and Ethylbenzene Functionalized Multiwall Carbon Nanotubes

Fabio Faraguna, Ante Jukić and Elvira Vidović*

University of Zagreb, Faculty of Chemical Engineering and Technology, Marulićev trg 19, HR-10 000, Croatia

Abstract: Polystyrene nanocomposite materials prepared with differently functionalized multiwall carbon nanotubes (CNT) as nanofillers were investigated. Two types of functionalized multiwall carbon nanotubes were used: oxidized (CNT-COOH) and their ester analogue with ethylbenzene groups (CNT-COOEtBz) introduced by further functionalization of the fore. The functionalized nanotubes were examined by thermogravimetric analysis and contact angle method that both revealed differences between them. Also, their dispersion was investigated in polar methanol and non-polar toluene with the assistance of UV-Vis spectrophotometer. Good dispersion of CNT-COOH in methanol and CNT-COOEtBz in toluene is in accordance with polarity introduced on the surfaces of carbon nanotubes. Mixtures of styrene monomer and 1 wt. % of CNT-COOH or CNT-COOEtBz in toluene were reacted in a radical *in-situ* polymerization reaction in order to prepare corresponding nanocomposites. Prior to the reaction nanotubes were dispersed by sonication of the reaction mixture. The synthesized composites were characterized by the SEC, TGA, DSC, DMA, SEM and contact angle method. The DSC measurements show a significant T_g shift towards lower temperature since T_g of studied PS is around 60 °C and T_g of PS composites with CNT-COOH at 35 °C and CNT-COOEtBz at 33 °C. The storage modulus increase in the PS/CNT-COOEtBz composite can be assigned to a larger similarity of matrix and filler structure. This is corroborated with the SEM micrographs where much lesser extent of agglomeration can be seen.

Keywords: Contact angle, dispersibility, loss factor, storage module, thermal stability.

1. INTRODUCTION

Polymer materials have changed our life style over the last 60 years immensely, so much that it can be considered revolutionary. And their expansion into new and more complex and demanding areas of application continue. One very important area of their application is the composite materials where polymer composites take a prominent place. Because composite materials can be the answer to ever increasing demand for materials of exceptional quality, multi-purpose and multifunctional materials for various applications in the industry. Among the most extensively used nanofillers are those belonging to the class of aluminum silicates, calcium carbonate, silicon dioxide, titanium dioxide, zinc oxide, as well as metal nanoparticles (Ag, Au, Cu, Rh, Pd) [1-3], which can further be differentiated by means of processing method, shapes, geometry, etc. Also, along with many other fillers carbon nanotubes (CNTs) are often used. Primarily, because carbon nanotubes exhibit a wide range of excellent mechanical, electrical, magnetic, and optical properties as well as nanometer scale diameter and high aspect ratio, along with chemical stability. This make them an ideal e.g. reinforcing agent for high strength polymer composites since their mechanical properties, such as Young's modulus and tensile strength, considerably

exceed those of currently available materials [4]. The research in this area started with Ajayan *et al.* [5] who has reported the first polymer nanocomposites using CNTs as a filler. Afterwards, different polymer/CNT nanocomposites have been prepared by incorporating CNTs into various polymer matrices, such as thermoplastics [6, 7], thermosetting resins [8, 9], liquid crystalline polymers [10], water-soluble polymers [11], conjugated polymers [12], to name just some examples. However, besides their extraordinary properties that provoked intense research activity, there are some characteristics that cause problems detected while preparing and formulating nanostructured composites based on CNT. It is extremely difficult to disperse and align CNTs in a polymer matrix because they usually form stabile bundles due to Van der Waals interactions. Therefore, the biggest issues in the preparation of CNT-reinforced composites is how to achieve an efficient dispersion of CNTs in a polymer matrix, the assessment of the dispersion, as well as the alignment of the CNTs in the matrix. Several methods are used for the dispersion of nanotubes in the polymer matrix such as melt-compounding or solution mixing, *in-situ* polymerization, etc. Additionally, the issue of dispersion and agglomeration of carbon nanotubes can be dealt dually by the procedure of nanocomposites preparation or modification of interactions between filler and matrix. Here, covalent or non-covalent modification of nanotubes can be used in order to improve interactions. It is known from the literature [13-20] that

*Address correspondence to this author at the University of Zagreb, Faculty of Chemical Engineering and Technology, P. O. Box 177, HR-10000 Zagreb, Croatia; Tel: + 385 1 45 97 128; Fax: + 385 1 45 97 142; E-mail: evidov@fkit.hr

by covalent functionalization of CNTs their solubility as well as dispersion in solvents and polymer can improve. Generally, covalent functionalization can be accomplished by direct reagents to the side walls of nanotubes or by modification of the groups bounded on the surface, in our case carboxylic acid groups. The presence of carboxylic acid groups on the nanotube surface is more convenient than others because a variety of chemical reactions can be carried out with this group. The presence of $-\text{COOH}$ groups on the nanotube surface enables the attachment of both inorganic and organic materials [21] but we have introduced ethylbenzene groups in order to evidence interaction of covalently functionalized CNTs with resembling polystyrenic matrix, since polystyrene belongs among four common plastic materials and is often used polymer matrix.

2. MATERIALS AND METHODS

2.1. Materials

Oxidized multiwall CNT from Chengdu Organic Chem. Co., Chinese Academy of Sciences, were used as received. The characteristics of used oxidized CNT are: diameter from 10 to 30 nm, purity > 90 %, length from 10 to 30 μm and COOH content 1.55 wt. % (share of surface carbon atom: 8-10 mol. %). In functionalization reaction sodium hydroxide pellets (98 %, Kemika), (2-bromoethyl)benzene (97 %, Fluka), hexadecyltrimethylammonium bromide (98 %, Sigma Aldrich) and demineralized water were used. For the purification of obtained functionalized CNT-COOEtBz, chloroform (99 %, Carlo Erba Reagenti), methanol (99.5 %, Carlo Erba Reagenti) and demineralized water were used. In the polymerization reactions styrene monomer (ST, polymerization grade, Fluka), 1,1-di(tert-butylperoxy)-3,3,5-trimethylcyclohexane (Trigonox 29[®], Akzo Chemie) as an initiator and toluene (p. a., Carlo Erba Reagenti) as a solvent were used. Mentioned solvents were also used in UV-Vis measurements.

2.2. Reaction of Functionalization of CNT-COOH into CNT-COOEtBz

Water solution of sodium hydroxide (250 ml, 6 mM NaOH) is added to oxidized multiwall carbon nanotubes (CNT-COOH, 1.55 wt. % COOH, 3 g) dropwise during 5 min with vigorous stirring. Additional mixing in ultrasonic bath is required (40 kHz, 30 min). Afterwards, during 5 minutes 20 ml of 6 mM NaOH solution that contains 500 mg of (2-bromoethyl)benzene and 100 mg of hexadecyltrimethylammonium bromide have been added dropwise in the flask. The reaction is allowed to proceed for 20 h, whereat 5 h at

the reflux temperature. Prepared CNT-COOEtBz have been separated by vacuum filtration and subsequently washed with chloroform, methanol and demineralized water. Afterwards, CNT-COOEtBz were dried in a vacuum oven 48 hours at 50 °C. Resulting CNT-COOEtBz are characterized by TGA, contact angle and UV-Vis measurements in order to prove effectiveness of functionalization procedure. Thermogravimetric analysis (TGA) was performed by TGA Q500 V20.13 Build 39 instrument at a heating rate of 10 °C min⁻¹ in a temperature range from room temperature up to 900 °C, in an inert atmosphere of nitrogen. Sample mass was around 4 mg. Contact angle measurements were performed by OCA 200 Data Physics Contact Angle System. Water droplets (6 μl) were placed on the surface of different CNT films. These films were prepared *via* deposition of dispersion of nanotubes in chloroform on the glass surface at room temperature. Contact angle of water on the pure glass surface was 50.7 °. Contact angle was measured after 10-15 s of contact between fluid and examined surface. Dispersion behavior of different CNTs in methanol and toluene were studied and quantified by using UV-Vis spectroscopy. Concentrations of nanotubes in the corresponding solvent from 10 to 50 mg L⁻¹ in the step of 10 mg L⁻¹ were prepared in the flasks that are further mixed using ultrasonic bath for two hours. After ultrasonic mixing UV-Vis measurements were undertaken within 10-15 minutes. Absorption of individually dispersed CNTs in methanol and toluene was measured with Shimadzu UV-1650 PC spectrophotometer operating between 400 and 700 nm.

2.3. Preparation and Characterization of Polystyrene Nanocomposites

Styrene (40 g) was weighed in Erlenmeyer flask and 1 wt. % of carbon nanotubes was added. The mixture was ultrasonically stirred in ultrasonic bath (40 kHz, 15 minutes) and afterwards poured in a preheated reactor (50 °C). Toluene (60 g) was added and the resulting mixture was homogenized with ultrasound probe (3 times for 30 seconds). Initiator 1,1-di(tert-butylperoxy)-3,3,5-trimethylcyclohexane, 1 wt. % with respect to the mass of the monomer was added and mixture was heated to 105 °C. After reaching the set temperature the reaction was allowed to proceed for six hours in a nitrogen atmosphere. A batch reactor of 250 ml of volume, double jacked using oil as a heat exchanger was used. The reaction mixture was stirred with anchor mixer at 150 rpm. After the reaction completion the resulting polymer bulk was poured into the Teflon molds and placed for drying in an oven at 60 °C till the constant weight.

Average molecular weights and polydispersity of polystyrene (PS) homopolymer and PS matrix from nanocomposite systems were determined by Polymer Laboratories GPC 20 instrument. Approximately 30 mg of sample was dissolved in 6 ml of toluene and introduced for chromatographic analysis. Solutions of nanocomposite samples had been vacuum filtered through filter paper before measurements to remove the nanotubes. Stationary phase was poly(styrene-co-divinylbenzene) copolymer gel of the particle size 3-100 μm , mobile phase was toluene, flow rate of 1 ml min^{-1} and detector was a photosensitive cell. Thermogravimetric analysis (TGA) was performed by TGA Q500 V20.13 Build 39 instrument at a heating rate of 10 $^{\circ}\text{C min}^{-1}$ in a temperature range from room temperature to 600 $^{\circ}\text{C}$ for pure polystyrene and to 900 $^{\circ}\text{C}$ for nanocomposites, in air. Mass of examined samples was around 15 mg. Differential scanning calorimetry (DSC) analysis was performed by DSC823e Mettler Toledo instrument. Masses of examined samples were 9-12 mg. Three heat-cool-heat runs were performed whereat heating and cooling rates were 10 $^{\circ}\text{C min}^{-1}$. Heating data for the second scan were used. Dynamic mechanical analysis (DMA) was performed by DMA 983 TA Instruments. The size of test specimens was ca. length 50 mm, width 10-13 mm, thickness ca. 2 mm. A constant frequency of jaw motion 1 Hz, 0.2 mm amplitude, a temperature interval from -30 $^{\circ}\text{C}$ to 80 $^{\circ}\text{C}$ at a heating rate of 5 $^{\circ}\text{C min}^{-1}$ were applied. Scanning electron microscopy (SEM) recording was carried out by VEGA 3 TESCAN microscope, with a detector of secondary electrons. All samples were previously sputter coated with Au or Pd in the argon plasma to enhance their conductivity. Contact angle measurements were performed by OCA 200 Data Physics Contact Angle System. Water droplets (2 μl) were placed on the surface of nanocomposites and contact angle was measured after 10-15 s of contact between fluid and examined surface.

3. RESULTS AND DISCUSSION

3.1. Functionalization of Oxidized into Ethylbenzene Ester Multiwall Carbon Nanotubes

The reaction pathway of CNT-COOH modification is shown in Figure 1. In the first step carboxylic groups of

oxidized CNTs were converted into sodium salt form, which in the next step reacted with (2-bromoethyl)-benzene giving corresponding CNT-COOEtBz ester. Similar reaction pathway was previously used by Wang *et al.* [22]. In literature the esterification reaction has been also commonly done using thionyl chloride [23-27] and *N,N'*-dicyclohexylcarbodiimide [28-30].

3.2. Characterization of Ethylbenzene Ester Multiwall Carbon Nanotubes

Thermogravimetric analysis is often used to determine the extent of functionalization and influence of functionalization on thermal stability of CNT [22, 27, 31, 32]. Here, thermal stability of functionalized multiwall carbon nanotubes measured in inert atmosphere of nitrogen has displayed a significant difference between the two kinds of nanotubes (Figure 2). The total weight change of CNT-COOH is much smaller while CNT-COOEtBz exhibit much more intensive weight loss. Thus, the total weight loss in former nanotubes amounts less than 4 wt. % (up to 900 $^{\circ}\text{C}$) while the latter such a loss display below 600 $^{\circ}\text{C}$ and the total loss higher than 10 wt. %. Bulkier ethylbenzene ester group attached onto nanotubes show lower stability, which results with higher fraction of volatile components.

The surface wettability of modified CNTs was quantified by contact angle measurements with water droplets. Contact angle values and corresponding photographs measured on CNT films and pure glass (measured for comparison reasons) are given in Table 1. Measurements of contact angle reveal a large difference in the surface properties of nanotubes with carboxyl functional groups and ethylbenzene ester group. Water droplets in contact with the surface of CNT-COOH display immediate seepage which points to a strong surface hydrophilicity as a result of interactions with the polar carboxylic groups. This behaviour is consistent with the literature data [22, 27]. On the other hand, in case of CNT-COOEtBz water droplets display a contact angle of 141.1 $^{\circ}$. This high angle is a result of increased hydrophobicity due to the introducing of nonpolar groups onto the surface of nanotubes.

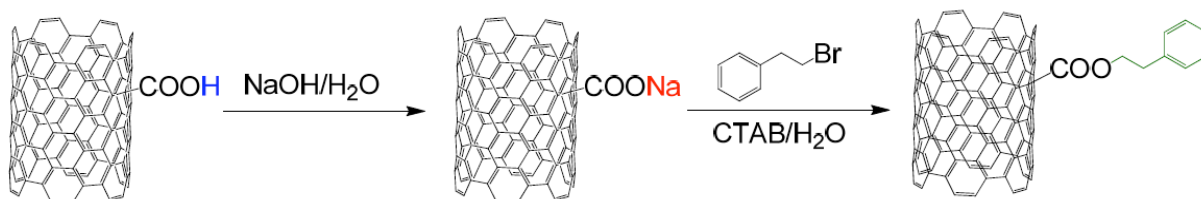


Figure 1: Reaction of CNT-COOH with NaOH and further functionalization with (2-bromoethyl)benzene into CNT-COOEtBz.

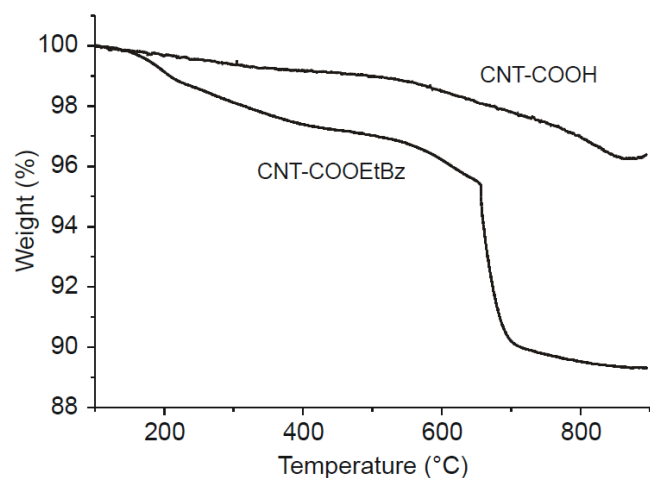
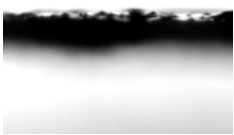


Figure 2: TGA of functionalized nanotubes measured at a heating rate of $10\text{ }^{\circ}\text{C min}^{-1}$ in an inert atmosphere of nitrogen.

Table 1: Pictures and Values of Contact Angle of Water Droplets on the Examined Surfaces

Sample	Shape of water droplets	Contact angle
Pure glass		50.7°
CNT-COOH		Seepage
CNT-COOEtBz		141.1°

Chemical functionalization of carbon nanotubes influences their dispersibility in solvents, among other properties. As a result, tailoring of this ability in organic solvents and water enables improvement of their compatibility with other materials, facilitating the preparation of composites [33,34]. Functionalization not only facilitates carbon nanotubes manipulation by various processes (mixing, blending, ultrasonic dispersing) but also allows tuning of their chemical and physical properties for specific demands and applications. After mixing of functionalized nanotubes (concentration of 0.1 wt. %) with water per hand, it was

observed that oxidized nanotubes fell to the bottom, while those modified with ethylbenzene remained on the surface due to their hydrophobicity (Figure 3).

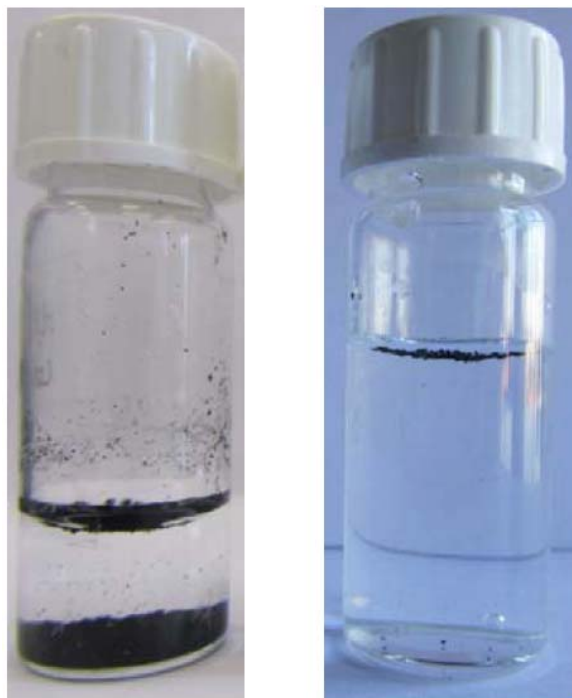


Figure 3: Behaviour of functionalized nanotubes (0.1 wt. %) CNT-COOH (left) and CNT-COOEtBz (right) in water after mixing per hand.

Also, dispersions of nanotubes were investigated in methanol and toluene. Methanol was selected as a polar solvent, while toluene was selected as a non-polar solvent. Nanotubes were dispersed in the selected solvent using ultrasonic bath during 2 hours. Dispersibility was measured by a UV-Vis spectrophotometer, whereat the concentration of dispersed nanotubes was counted *via* molar extinction coefficient, which is $\epsilon_{500} = 28.6\text{ cm}^2\text{ mg}^{-1}$ at 500 nm [35]. Quality of dispersion is expressed with the dispersibility index (DI), which is defined as:

$$DI = c_{UV} \times 100 / c$$

where c is the concentration of added CNTs and c_{UV} the concentration of individually dispersed nanotubes from UV-Vis measurements.

Dispersibility index of both kinds of nanotubes in toluene and methanol are shown in Figures 4 and 5, respectively. The calculated values of the dispersibility index slightly over 100 % can be explained either as a consequence of ultrasonic mixing where the possibility of pulling or breaking of nanotubes cannot be excluded, which finally leads to their increased number or as a consequence of experimental error during the samples

preparation. Regarding dispersion of CNT-COOH nanotubes in toluene (Figure 4) one can see that as the concentration increases from 10 mg L^{-1} to 50 mg L^{-1} the dispersibility index decreases from ca. 60 % to 15 %. On the other hand, CNT-COOEtBz display an opposite behavior, being placed in a solvent of similar polarity where increase in their concentration leads to the increase of dispersibility index (from 80 % up to 100 %), except for the highest concentration where a marked decrease of index is observed (45 %). Figure 5 shows dispersibility index of both kinds of nanotubes in methanol. Again, a significant difference between two systems regarding the index vs. concentration dependence can be observed. The dispersions of CNT-COOH show similar dispersibility index (90%-100%) for all examined concentrations. Although the highest index is recorded for the lowest concentration, with the further concentration increase the dispersibility index remain high, above 90 %. However, the dispersibility index of CNT-COOEtBz being placed in a solvent of opposite polarity decreases from ca. 70 % down to 20 % as their concentration increases.

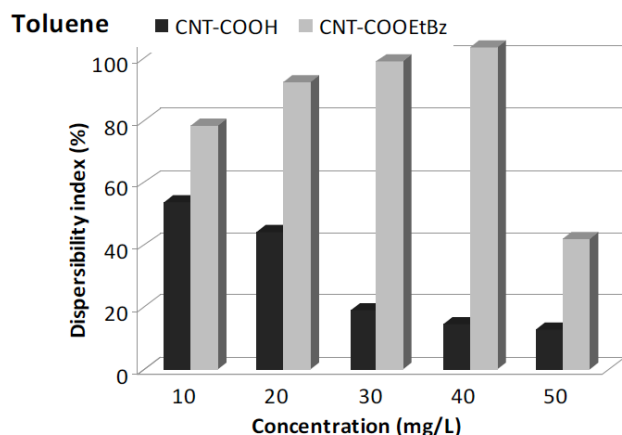


Figure 4: Dependence of dispersibility index on the concentration of CNT-COOH and CNT-COOEtBz in toluene.

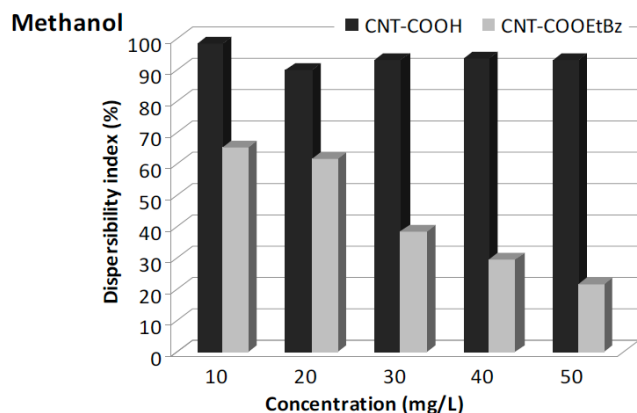


Figure 5: Dependence of dispersibility index on the concentration of CNT-COOH and CNT-COOEtBz in methanol.

In both cases one can see that the dispersibility of nanotubes depends strongly on interactions between functional groups on the CNT surface and a solvent surrounding them. The dispersibility of functionalized nanotubes is much higher if they are mixed with a solvent of similar polarity compared with a solvent of opposite polarity. As the concentration increases the dispersibility decreases in solvent of opposite polarity because the interactions between carbon nanotubes are more pronounced and they tend to agglomerate. However, interactions between carbon nanotubes are less pronounced in a solvent of similar polarity, but if the critical concentration has been exceeded, like in case of CNT-COOEtBz in toluene, agglomeration of nanotubes becomes a dominant effect and, therefore the dispersibility decreases with the concentration increase.

3.3. Polystyrene Composites with Oxidized and Ethylbenzene Ester Multiwall Carbon Nanotubes

There is a very intensive research activity regarding composites of carbon nanotubes in polymer matrix based on polystyrene and its copolymers. In most of the cases solution processing or melt-blending [36-38] is used as a common method of composites preparation. However, the researches that include synthesis of polystyrene matrix are scarce and are mainly related to the specific polymerization procedures [39-41]. Here, two kinds of polystyrene composites with oxidized and ethylbenzene ester multiwall carbon nanotubes as fillers are prepared by *in-situ* polymerization. Afterwards, the obtained nanocomposites are characterized.

The compatibility of the CNTs and monomer can affect polymerization. There are conflicting findings in the literature [42-44], about the impact of carbon nanotubes present in the reaction mixture on the molecular weights and polydispersity index of resulting polymeric matrix. It depends on monomer and initiator type, polymerization conditions, as well as surface area and quality of the nanotubes. Thus, Seppälä *et al.* [44] have found that in emulsion polymerization of styrene, multiwall CNTs increased the molar mass. The increase of molar mass was based on the compatible molecular structures of CNTs and styrene, so that individual nanotubes were covered by monomer clouds when initiator arrived. The CNTs stabilized the emulsions, and molar mass distributions narrowed with higher amounts of CNTs. In combined emulsion/suspension polymerization of styrene, CNTs reacted with the initiator and there was less initiator to polymerize the monomer.

Table 2: Molar Weight Averages and Polydispersity Index of Polystyrene (PS) and its Composites

Sample	M_n / g mol ⁻¹	M_w / g mol ⁻¹	M_z / g mol ⁻¹	PD
PS (non-filtered)	24400	49900	85100	2.04
PS (filtered)	24600	49100	82200	2.00
PS/CNT-COOH	29200	55300	89500	1.89
PS/CNT-COOEtBz	35500	69300	115400	1.95

Homopolymerization of styrene and both its composites were performed under the same conditions in order to determine the effect of present nanotubes on the final structure of polystyrene matrix. Prior to GPC/SEC measurements solution of composites was filtered (in order to remove CNTs). For the comparison reason, solution of pure PS was filtered, as well. Figure 6 shows obtained chromatographs and values of number (M_n) and weight (M_w) averages as well as polydispersity index (PD) are given in Table 2. There is no any significant difference between values for pure polystyrene before and after filtration. This finding bespeaks as valid values obtained for the prepared composites after filtration. It is evident that the presence of nanotubes in PS/CNT-COOH causes increase in M_n (19%) and M_w (13%) but reduces PD (5%), while even a greater increase of M_n (44%) and M_w (41%) with a negligible reduction of PD (2%) cause present nanotubes in PS/CNT-COOEtBz.

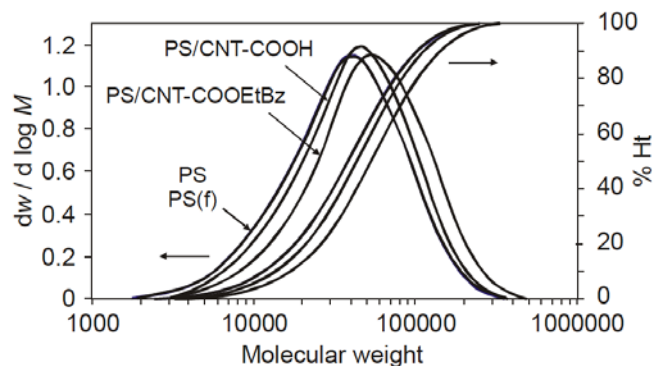


Figure 6: Chromatographs of polystyrene (PS) before and after filtration (f) and PS/CNT-COOH and PS/CNT-COOEtBz composites.

Thermal stability of synthesized PS/CNT-COOH or PS/CNT-COOEtBz composites was investigated by TG analysis. The obtained thermograms shown in Figure 7 display clearly that the addition of nanotubes does not have a significant impact on thermal stability of nanocomposites with respect to the pure polymer. It is noted that all three systems show major thermal decomposition in one step at temperatures above 300 °C. Furthermore, in the area of weight loss of up to 5 % PS and PS/CNT-COOH composite behave alike, the

loss occurs at temperature 223 °C and 241 °C, respectively. But the PS/CNT-COOEtBz shows a larger initial instability which is probably associated with somewhat larger amount of residual styrene or toluene due to the favorite interaction with CNT-COOEtBz. This composite exhibits a weight loss of 5 % at temperature as low as 175 °C while in the range 225 °C to 240 °C the loss exceeds 10 %.

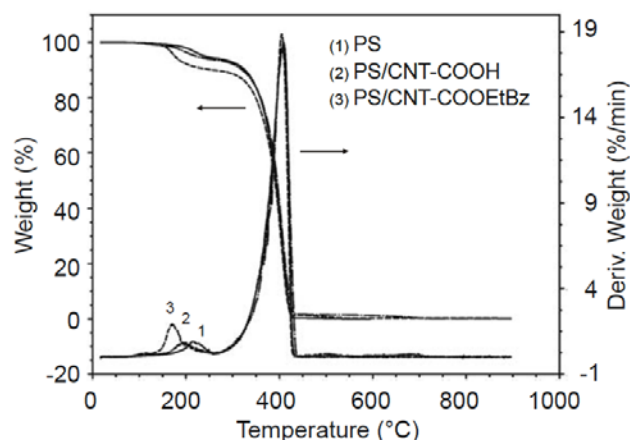


Figure 7: Thermal stability of PS (1), PS/CNT-COOH (2) and PS/CNT-COOEtBz (3) measured at a heating rate of 10 °C min⁻¹ in air.

Figure 8 shows thermographs of the final stage of thermal decomposition as an evidence of nanotubes

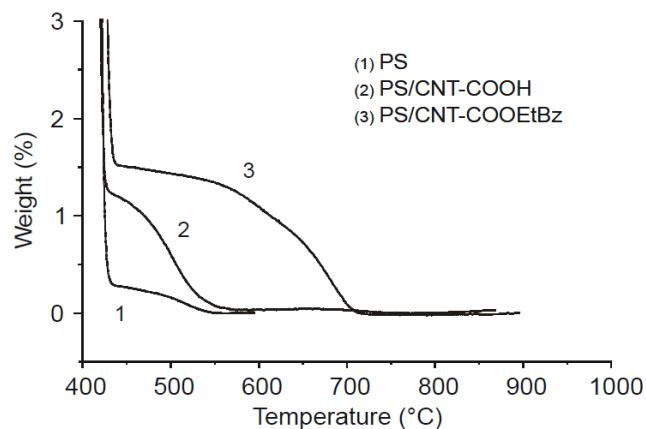


Figure 8: Thermographs of the final stage of thermal decomposition of PS (1), PS/CNT-COOH (2) and PS/CNT-COOEtBz (3) composites.

combustion. It can be seen that complete decomposition of PS and PS/CNT-COOEtBz composite appear at the similar temperature around 550 °C. However, in the PS/CNT-COOH composite it happens at temperature above 700 °C, which indicates higher stability of nanotubes oxidized with carboxylic groups. Also, from these data a share of nanotubes in nanocomposites can be calculated. Calculations of the mass remaining after decomposition of the majority of polymer matrix (around 440 °C) and subtracting the mass of PS residue, give 1.21 % in PS/CNT-COOH and 0.93 % in PS/CNT-COOEtBz, both matching the theoretical value of 1 wt. %. Here, the initial decomposition step is not taken into consideration.

The DSC thermal curves of pure polystyrene, PS/CNT-COOH and PS/CNT-COOEtBz nanocomposites are shown in Figure 9. One can see that the addition of modified multiwall carbon nanotubes affects significantly the glass transition temperature (T_g) of styrene homopolymer. In comparison to pure PS the composites display the T_g shift downwards of about 25 °C, though the T_g values in both composites are similar, within 2 °C. The T_g shift indicates that the addition of 1 wt. % of nanotubes causes the plasticizer effect and enhances movement of macromolecular chains. Also, thermal conductivity of nanocomposites [45] is improved, which enables a faster input of energy within the sample, and is another reason for the T_g lowering.

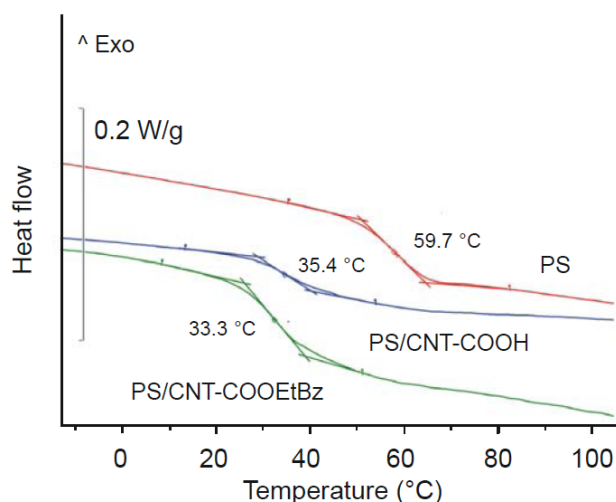


Figure 9: DSC thermal curves of heat flow vs. temperature for: PS, PS/CNT-COOH and PS/CNT-COOEtBz composites.

In order to complement the information provided by the traditional techniques of thermal analysis, DSC and TGA, dynamic mechanical analysis of materials was applied, too. DMA was performed in a temperature range from -30 °C to 80 °C to investigate mechanical

properties of studied materials and further understand the influence of carbon nanotubes. Figure 10 shows that in the temperature range from -30 °C to room temperature there is a big difference in storage modulus (E') between the two composites. Thus, PS/CNT-COOEtBz shows approximately twice as high storage modulus as PS/CNT-COOH composite while E' modulus of pure PS lies in the middle. In that temperature range PS/CNT-COOEtBz are stronger associated with the polymer matrix due to the similar polarity and the possibility of additional π - π interactions between the benzene groups of polystyrene and those on nanotubes, which increases storage modulus. On contrary, the polar COOH groups of oxidized nanotubes display poor interactions with polymer matrix because of different polarity that result in the storage modulus decrease in comparison with pure PS. However, as the temperature rises, these interactions become weaker and consequently the effect of nanotubes functionalization on the improvement / worsening of the storage modulus vanishes.

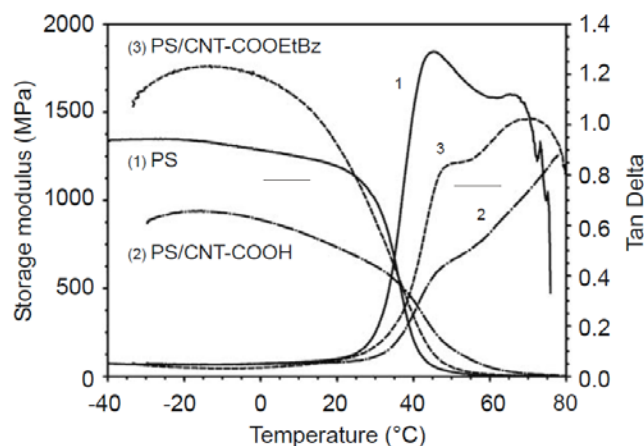


Figure 10: DMA analysis of PS (1), PS/CNT-COOH (2) and PS/CNT-COOEtBz (3) composites: (left) storage modulus (E'), (right) angle of phase shift ($\tan \delta$).

Polystyrene having loss modulus (E'') of 330 MPa surpasses almost three times both its composites (Table 3). But T_g values drawn from E'' are relatively close in all three materials (36.3, 42.3 and 39.6 °C). However, both composites display a shift towards higher T_g relative to polystyrene as opposite to what was recorded by DSC measurements. At the same time, polystyrene displays T_g at 36 °C that is much lower compared to 60 °C recorded by DSC. All this indicates the differences between the various methods.

Figure 10 shows the angles of phase shift ($\tan \delta$), which represents the ratio of the energy loss due to friction and the maximal potential energy that is stored in the examined material. One can see that the $\tan \delta$

Table 3: Values of Loss Module (E'') of PS, PS/CNT-COOH and PS/CNT-COOEtBz Composites at Various Temperatures.

Sample	PS	PS/CNT-COOH	PS/CNT-COOEtBz
E'' (-20 °C) / MPa	63	46	63
E'' (0 °C) / MPa	66	44	61
E'' (20 °C) / MPa	83	41	85
E'' (T_g) / MPa	330 (36.3 °C)	115 (42.3 °C)	130 (39.6 °C)
E'' (60 °C) / MPa	8	30	12

increases significantly only beyond the glass transition temperature, after the increase in the mobility of kinetic units takes place. The ability of material to store or dissipate energy can be estimated based on plotted curves. Polystyrene displays the highest values of $\tan \delta$ over a broad range of temperature from 20 °C to 70 °C with a maximum higher than 1.2 around 40 °C. PS/CNT-COOEtBz exhibit similar behavior apart from that its maximum barely exceeds 1.0 and is shifted towards higher temperature (70 °C). A high angle of phase shift of a material does not necessarily mean that it is the material of choice, because the attention should be paid to each module separately. Very good materials for the energy storage (noise and vibration absorption) are those with both high storage module, as well as the $\tan \delta$.

The surface properties of composites were investigated by measuring contact angle, which has clearly shown the effect of the addition of nanotubes. Thus, the PS/CNT-COOEtBz shows a decrease of contact angle of only 3 °, while in PS/CNT-COOH a more pronounced reduction of 16 ° relative to the contact angle of pure polystyrene occurs (Table 4). The latter material is an obvious example of the hydrophilicity increase due to introduction of hydrophilic nanotubes in the system, even in as small quantities as 1 wt. % (cf. Tab. 1).

Table 4: Values of Contact Angle of Examined Materials

Sample	Contact angle / °
PS	93.8 ± 3.1
PS/CNT-COOH	78.0 ± 4.3
PS/CNT-COOEtBz	90.7 ± 2.5

In order to determine the quality of the dispersion and the extent of agglomeration of modified nanotubes in polystyrene matrix SEM images were taken. In both samples a fairly good homogeneous distribution of

nanotubes can be seen, whereat nanotubes in images are presented as bright dots or dashes (Figure 11). In the PS/CNT-COOH composite (Figure 11a and b) small areas of agglomeration appear, while in the PS/CNT-COOEtBz the areas of agglomeration were not observed even at a higher magnification (Figure 11c and d). Nanotubes in PS/CNT-COOH can be seen at lower magnifications (Figure 11a) because they have been pulled out of the polymer matrix to a large extent. In PS/CNT-COOEtBz it is difficult to spot nanotubes (Figure 11c) though at a higher magnification they can be seen as bright dots (Figure 11d). These phenomena indicate that upon the brittle fracture of sample in case of PS/CNT-COOH pulling of nanotubes from the polymer matrix occurs due to weaker interaction while in PS/CNT-COOEtBz the pulling is less pronounced because of better interaction.

CONCLUSION

Reaction of covalent functionalization of CNT-COOH with NaOH and further with (2-bromomethyl)-benzene into CNT-COOEtBz was successfully performed, whereupon they display different behavior when characterized by thermogravimetric analysis and contact angle measurements. Also, undertaken UV-Vis measurements show distinctive dispersibility of functionalized nanotubes in polar methanol and non-polar toluene.

Furthermore, composites of CNT-COOH or CNT-COOEtBz and polystyrene matrix are prepared and characterized. The addition of modified multiwall carbon nanotubes affects significantly the glass transition temperature (T_g) of styrene homopolymer, which results with T_g downwards shift of ca. 25 °C relative to pure PS in both composites. Two composites display a big difference in storage modulus (E'). The PS/CNT-COOEtBz shows approximately twice as high storage modulus as PS/CNT-COOH composite due to the similar polarity and the possibility of additional π - π interactions between the benzene

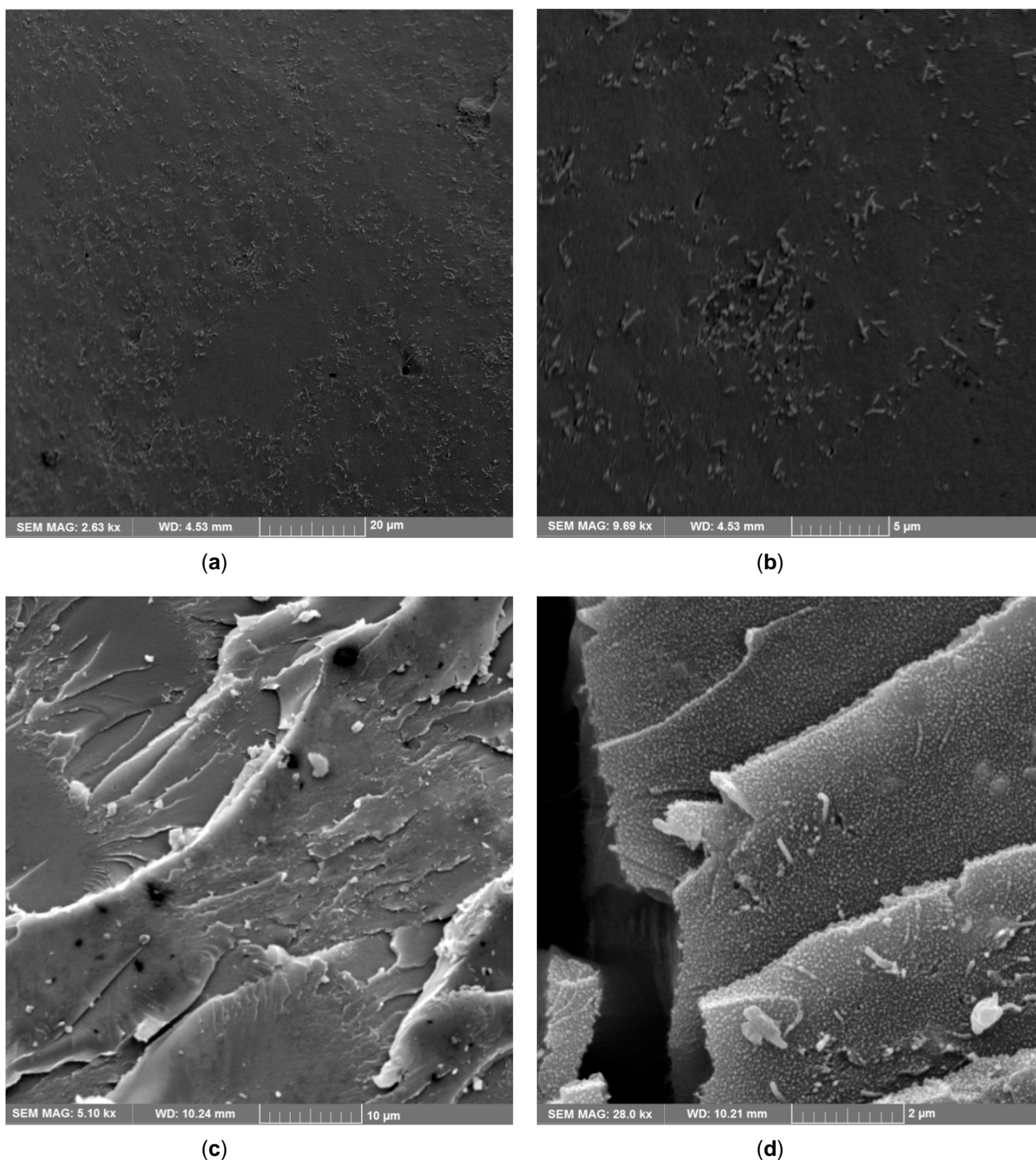


Figure 11: Scanning electron microscopy of PS/CNT-COOH at a magnification of 2.63 kx (a) and 9.69 kx (b), and PS/CNT-COOEtBz at a magnification of 5.10 kx (c) and 28.00 kx (d).

groups of polystyrene and those on nanotubes. Also, the contact angle measurements display differences between two composites where the PS/CNT-COOEtBz showed a decrease of only 3° , while in PS/CNT-COOH a more pronounced reduction of 16° relative to the contact angle of pure polystyrene was noticed. SEM micrographs of both composites display a fairly good homogeneous distribution of nanotubes, though it is better in the PS/CNT-COOEtBz because the areas of agglomeration were not observed even at a higher

magnification. Also, upon the brittle fracture of the PS/CNT-COOEtBz sample the pulling is less pronounced due to better interaction between nanotubes and the polymer matrix.

ACKNOWLEDGEMENTS

These materials are based on work financed by the Croatian Foundation for Science and Ministry of Science of the Republic of Croatia.

REFERENCES

- [1] Wang Q, Chen G, Alghamdi AS. Influence of nanofillers on electrical characteristics of epoxy resins insulation. In: 2010 IEEE International Conference on Solid Dielectrics, Potsdam, Germany, 4 - 9 Jul 2010. IEEE: 263-6.
- [2] Singha S, Thomas MJ. Dielectric properties of epoxy nanocomposites. *IEEE Trans Dielectr Electr Insul* 2008; 15(1): 12-23. <http://dx.doi.org/10.1109/T-DEI.2008.4446732>
- [3] Wang Q, Chen G. Effect of nanofillers on the dielectric properties of epoxy nanocomposites. *Adv Mater Res* 2012; 1(1): 93-107. <http://dx.doi.org/10.12989/amr.2012.1.1.093>
- [4] Fidelus JD, Wiesel E, Gojny FH, Schulte K, Wagner HD. Thermo-mechanical properties of randomly oriented carbon/epoxy nanocomposites. *Compos A* 2005; 36: 1555-61. <http://dx.doi.org/10.1016/j.compositesa.2005.02.006>
- [5] Ajayan PM, Stephan O, Colliex C, Trauth D. Aligned carbon nanotube arrays formed by cutting a polymer resin-nanotube composite. *Science* 1994; 265: 1212-4. <http://dx.doi.org/10.1126/science.265.5176.1212>
- [6] Iijima S. Helical microtubules of graphitic carbon. *Nature* 1991; 354: 56-58. <http://dx.doi.org/10.1038/354056a0>
- [7] Seo MK, Park SJ. Electrical resistivity and rheological behaviors of carbon nanotubes-filled polypropylene composites. *Chem Phys Lett* 2004; 395: 44-8. <http://dx.doi.org/10.1016/j.cplett.2004.07.047>
- [8] Bachtold A, Hadley P, Nakanishi T, Dekker C. Logic circuits with carbon nanotube transistors. *Science* 2001; 294: 1317-20. <http://dx.doi.org/10.1126/science.1065824>
- [9] Gojny FH, Wichmann MHG, Fiedler B, Schulte K. Influence of different carbon nanotubes on the mechanical properties of epoxy matrix composites-A comparative study. *Compos Sci Technol* 2005; 65: 2300-13. <http://dx.doi.org/10.1016/j.compscitech.2005.04.021>
- [10] Kasumov AY, Deblock R, Kociak M, Reulet B, Bouchiat H, Khodos I, et al. Supercurrents through single-walled carbon nanotubes. *Science* 1999; 284:1508-11. <http://dx.doi.org/10.1126/science.284.5419.1508>
- [11] Baughman RH, Cui C, Zakhidov AA, Iqbal Z, Barisci JN, Spinks GM, et al. Carbon nanotube actuators. *Science* 1999; 284: 1340-4. <http://dx.doi.org/10.1126/science.284.5418.1340>
- [12] Niu C, Sichel EK, Hoch R, Moy D, Tennet H. High power electrochemical capacitors based on carbon nanotube electrodes. *Appl Phys Lett* 1997; 70: 1480-2. <http://dx.doi.org/10.1063/1.118568>
- [13] Holzinger M, Abraham J, Whelan P, Graupner R, Ley, L, Hennrich F, et al. Functionalization of single-walled carbon nanotubes with (R-) oxycarbonyl nitrenes. *J Am Chem Soc* 2003; 125: 8566-80. <http://dx.doi.org/10.1021/ja029931w>
- [14] Georgakilas V, Tagmatarchis N, Pantarotto D, Bianco A, Briand JP, Prato M. Amino acid functionalisation of water soluble carbon nanotube. *Chem Commun* 2002; 24: 3050 -1. <http://dx.doi.org/10.1039/b209843a>
- [15] O'Connell M J, Boul P, Ericson LM, Huffman C, Wang Y, Haroz E, et al. Reversible water-solubilization of single-walled carbon nanotubes by polymer wrapping. *Chem Phys Lett* 2001; 342(3-4): 265-71. [http://dx.doi.org/10.1016/S0009-2614\(01\)00490-0](http://dx.doi.org/10.1016/S0009-2614(01)00490-0)
- [16] Kim OK, Je J, Baldwin JW, Kooi S, Phehrsson PE, Buckley LJ. Solubilization of single-wall carbon nanotubes by supramolecular encapsulation of helical amylose. *J Am Chem Soc* 2003; 125(15): 4426-7. <http://dx.doi.org/10.1021/ja029233b>
- [17] Liu J, Rinzler AG, Dai H, Hafner JH, Tradley RK, Boul PJ, et al. Fullerene Pipes. *Science* 1998; 280: 1253-6. <http://dx.doi.org/10.1126/science.280.5367.1253>
- [18] Novais RM, Simon F, Pötschke P, Villmow T, Covas JA, Paiva MC. Poly(lactic acid) composites with poly(lactic acid)-modified carbon nanotubes. *J Polym Sci A: Polym Chem* 2013; 51: 3740-50. <http://dx.doi.org/10.1002/pola.26778>
- [19] Moore VC, Strano MS, Haroz EH, Hauge RH, Smalley RE, Schmidt J, et al. Individually suspended single-walled carbon nanotubes in various surfactants. *Nano Lett* 2003; 3: 1379-82. <http://dx.doi.org/10.1021/nl034524j>
- [20] Zhang X, Sreekumar TV, Liu T, Kumar S. Properties and structure of nitric acid oxidized single wall carbon nanotube films. *J Phys Chem B* 2004; 108: 16435-40. <http://dx.doi.org/10.1021/jp0475988>
- [21] Wu HX, Qiu XQ, Cao WM, Lin YH, Cai RF, Qian SX. Polymer-wrapped multiwalled carbon nanotubes synthesized via microwave assisted in situ emulsion polymerization and their optical limiting properties. *Carbon* 2007; 45: 2866-72. <http://dx.doi.org/10.1016/j.carbon.2007.10.009>
- [22] Xu D, Liu H, Yang L, Wang Z. Fabrication of superhydrophobic surfaces with non-aligned alkyl-modified multi-wall carbon nanotubes. *Carbon* 2006; 44: 3226-31. <http://dx.doi.org/10.1016/j.carbon.2006.06.030>
- [23] Alvaro M, Atienzar P, de la Cruz P, Delgado JL, Garcia H, Langa F. Synthesis and photochemistry of soluble, pentyl ester-modified single wall carbon nanotube. *Chem Phys Letters* 2004; 386(4-6): 342-5. <http://dx.doi.org/10.1016/j.cplett.2004.01.087>
- [24] Yun S, Im H, Heo Y, Kim J. Crosslinked sulfonated poly(vinyl alcohol)/sulfonated multi-walled carbon nanotubes nanocomposite membranes for direct methanol fuel cells. *J Membr Sci* 2011; 380(1-2): 208-15. <http://dx.doi.org/10.1016/j.memsci.2011.07.010>
- [25] Hill DE, Lin Y, Rao AM, Allard LF, Sun YP. Functionalization of carbon nanotubes with polystyrene. *Macromolecules* 2002; 35: 9466-71. <http://dx.doi.org/10.1021/ma020855r>
- [26] Baskaran D, Mays JW, Bratcher MS. Polymer adsorption in the grafting reactions of hydroxyl terminal polymers with multi-walled carbon nanotubes. *Polymer* 2005; 46: 5050-7. <http://dx.doi.org/10.1016/j.polymer.2005.04.012>
- [27] Fraguna F, Peter R, Volovšek V, Jukić A. Surface modification of multiwall carbon nanotubes by esterification reaction with methanol, butanol and dodecanol. *J Nanosci Nanotechnol* 2014; 14: 1-8.
- [28] Hennrich F, Lebedkin S, Malik S, Tracy J, Barczewski M, Rosner H, et al. Preparation, characterization and applications of free-standing single walled carbon nanotube thin films. *Phys Chem Chem Phys* 2002; 4(11): 2273-7. <http://dx.doi.org/10.1039/b201570f>
- [29] Sun YP, Huang W, Lin Y, Fu K, Kitaygorodskiy A, Riddle LA, et al. Soluble dendron-functionalized carbon nanotubes: preparation, characterization, and properties. *Chem Mater* 2001; 13(9): 2864-9. <http://dx.doi.org/10.1021/cm010069j>
- [30] Hamon MA, Hui H, Bhowmik P, Itkis HME, Haddon RC. Esterfunctionalized soluble single-walled carbon nanotubes. *Appl Phys A: Mater Sci Process* 2002; 74(3): 333-8. <http://dx.doi.org/10.1007/s003390201281>
- [31] Chen X, Tao F, Wang J, Yang H, Zou J, Chen X, et al. Concise route to styryl-modified multi-walled carbon nanotubes for polystyrene matrix and enhanced mechanical properties and thermal stability of composite. *Mater Sci Eng A* 2009; 499(1-2): 469-75. <http://dx.doi.org/10.1016/j.msea.2008.09.044>
- [32] Chen S, Shen W, Wu G, Chen D, Jiang M. A new approach to the functionalization of single-walled carbon nanotubes

- with both alkyl and carboxyl groups. *Chem Phys Lett* 2005; 402(4-6): 312-7.
<http://dx.doi.org/10.1016/j.cplett.2004.12.035>
- [33] Zeng L, Zhang L, Barron AR. Tailoring aqueous solubility of functionalized single-wall carbon nanotubes over a wide pH range through substituent chain length. *Nano Lett* 2005; 5(10): 2001-4.
<http://dx.doi.org/10.1021/nl0514994>
- [34] Banerjee S, Kahn MGC, Wong SS. Rational chemical strategies for carbon nanotube functionalization. *Chem Eur J* 2003; 9: 1898-908.
<http://dx.doi.org/10.1002/chem.200204618>
- [35] Rastogi R, Kaushal R, Tripathi SK, Sharma AL, Kaur I, Bharadwaj LM. Comparative study of carbon nanotube dispersion using surfactants. *J Colloid Interface Sci* 2008; 328: 421-8.
<http://dx.doi.org/10.1016/j.jcis.2008.09.015>
- [36] Al-Saleh MH, Al-Anid HK, Hussain YA. CNT/ABS nanocomposites by solution processing: Proper dispersion and selective localization for low percolation threshold. *Compos A Appl Sci Manuf* 2013; 46: 53-9.
<http://dx.doi.org/10.1016/j.compositesa.2012.10.010>
- [37] Gödel A, Kasaliwal GR, Pötschke P, Heinrich G. The kinetics of CNT transfer between immiscible blend phases during melt mixing. *Polymer* 2012; 53(2): 411-21.
<http://dx.doi.org/10.1016/j.polymer.2011.11.039>
- [38] Bose S, Mukherjee M, Pal K, Nayak GC, Das CK. Development of core-shell structure aided by SiC-coated MWNT in ABS/LCP blend. *Polym Adv Technol* 2010; 21(4): 272-8.
- [39] Yang Z, Donga B, Huang Y, Liu L, Yan FY, Li HL. Enhanced wear resistance and micro-hardness of polystyrene nanocomposites by carbon nanotubes. *Mater Chem Phys* 2005; 94: 109-13.
<http://dx.doi.org/10.1016/j.matchemphys.2005.04.029>
- [40] Khan MU, Gomes VG, Altarawneh IS. Synthesizing polystyrene/carbon nanotube composites by emulsion polymerization with non-covalent and covalent functionalization. *Carbon* 2010; 48(10): 2925-33.
<http://dx.doi.org/10.1016/j.carbon.2010.04.029>
- [41] Choi HJ, Zhang K, Lim JY. Multi-walled carbon nanotube/polystyrene composites prepared by in-situ bulk sonochemical polymerization. *J Nanosci Nanotechnol* 2007; 7(10): 3400-3.
<http://dx.doi.org/10.1166/jnn.2007.833>
- [42] Jia Z, Wang Z, Xu C, Liang J, Wei B, Wu D, *et al.* Study on poly(methyl methacrylate): carbon nanotube composites. *Mater Sci Eng A* 1999; 271: 395-400.
[http://dx.doi.org/10.1016/S0921-5093\(99\)00263-4](http://dx.doi.org/10.1016/S0921-5093(99)00263-4)
- [43] Park SJ, Cho MS, Lim ST, Choi HJ, Jhon MS. Synthesis and dispersion characteristics of multi-walled carbon nanotube composites with poly(methyl methacrylate) prepared by in-situ bulk polymerization. *Macromol Rapid Commun* 2003; 24: 1070-3.
<http://dx.doi.org/10.1002/marc.200300089>
- [44] Annala M, Lahelin M, Seppälä J. The effect of MWCNTs on molar mass in in situ polymerization of styrene and methyl methacrylate. *Eur Polym J* 2012; 48(9): 1516-24.
<http://dx.doi.org/10.1016/j.eurpolymj.2012.05.016>
- [45] Han Z, Fina A. Thermal conductivity of carbon nanotubes and their polymer nanocomposites: A review. *Prog Polym Sci* 2011; 36(7): 914-44.
<http://dx.doi.org/10.1016/j.progpolymsci.2010.11.004>

Received on 22-11-2013

Accepted on 04-12-2013

Published on 25-12-2013

DOI: <http://dx.doi.org/10.12974/2311-8717.2013.01.01.4>© 2013 Faraguna *et al.*; Licensee Savvy Science Publisher.

This is an open access article licensed under the terms of the Creative Commons Attribution Non-Commercial License (<http://creativecommons.org/licenses/by-nc/3.0/>) which permits unrestricted, non-commercial use, distribution and reproduction in any medium, provided the work is properly cited.